Indian J. Met. Hydrol. Geophys. (1976), **27**, 4, 397—408

551.513.1 : 543.422.4

Spectral representation of hemispheric flow patterns

H. S. BEDI

Meteorological Office, New Delhi

(*Received 9 May 1975*)

ABSTRACT. The method for representing hemispheric atmospheric flow patterns in terms of surface spherical harmonics is discussed. Spectral form of linear balance equation is derived and solved with a suitable boundary condition. The results show that the planetary scale atmospheric systems can be represented to a high degree of accuracy by a limited number of spherical harmonics. The stream function spectrum arrived at by solving spectral form of linear balance equation gives proper representation of actual atmospheric systems.

1. Introduction

During recent years, sufficient interest has been developed in the use of spectral methods for study of dynamics of large scale atmospheric systems. Theoretical as well as observational studies based on these methods have thrown much light on the non-linear dynamics of the atmosphere (Lorenz 1963, Saltzman and Fleisher 1960, Wiin-Nielsen 1964, 1967). Some spectral models for short and medium range prediction of atmospheric flow have also been developed (Robert 1966, Kurbatkin 1972). Till recently the development of spectral prediction models has been hampered due to difficulty in calculation and storage of large number of 'interaction coefficients'. However, recent works of Eliasen *et. al.* (1970) and Orszag (1971), have led to the development of a relatively simpler and straight forward method of calculating interaction terms. This has led to development of some sophisticated hemispheric and global spectral models (Bourke 1972, WMO 1974). For spherical or hemispherical domain, spherical harmonics are the appropriate orthogonal functions and have been used in these models. The success of these spectral models, whether for diagnostic or prognostic purposes depends much on the efficient representation of basic data by its spectral components. The purpose of the present study is to demonstrate the effectiveness of spherical harmonic spectral components in representing hemispheric geopotential field as well as derived stream function field which is commonly used as basic input in different atmospheric models.

2. Analysis procedure

At a given time, any scalar field 'h' at a constant height or pressure level is function of latitude θ and longitude λ. Any piecewise differentiable field over spherical domain, a condition which different meteorological fields like geopotential height are assumed to fulfil, can be represented to a desired degree of accuracy by superposition of a truncated series of spherical harmonic components so that

$$h(\mu, \lambda) = \sum_{m=-M}^{M} \sum_{n=|m|}^{|m|+J} A_n^m \, Y_n^m(\mu, \lambda) \quad (1)$$

$Y_n^m(\mu)$ is surface spherical harmonic of order m and degree n and

$$Y_n^m(\mu, \lambda) = P_n^m(\mu) \, e^{im\lambda} \quad (2)$$

$P_n^m(\mu)$ is normalised associated Legendre function of first kind and is given by

$$P_n^m(\mu) = \frac{1}{2^n \cdot n!} \left(\frac{2n+1}{2} \cdot \frac{(n-m)!}{(n+m)!} \right)^{1/2} \times (1-\mu^2)^{m/2} \frac{d^{n+m}(\mu^2-1)^n}{d\mu^{n+m}}$$

$$\text{for } n \geqslant m \quad (3)$$

and $P_n^m(\mu) = 0$ for $n < m$

where $\mu = \sin\theta$ and A_n^m is complex amplitude.

M and J determine the truncation of spherical harmonic spectrum.

It can be shown that

$$P_n^{-m}(\mu) = (-1)^m P_n^m(\mu) \quad (4)$$

$$\text{and } A_n^{-m} = (-1)^m A_n^{*m} \quad (5)$$

A_n^{*m} being the complex conjugate of A_n^m

For surface spherical harmonic representation of any real field it is necessary to include harmonics of order m as well as of $-m$ as has been done in (1).

Physically, $Y_n^m(\mu, \lambda)$ represents a two-dimensional wave on a spherical surface with m sinusoidal waves in the east-west direction along any latitude circle associated with factor $e^{im\lambda}$ and a polynomial representation having $n-m$ zeros (nodes) between north and south poles associated with factor $P_n^m(\mu)$. $P_n^m(\mu)$'s with even number of zeros between poles are symmetric with respect to equator whereas those having odd number of zeros are antisymmetric.

Normalised associated Legendre functions and spherical harmonics satisfy the following orthogonality conditions over a spherical domain and

$$\int_{-1}^{1} P_{n1}^m(\mu) \cdot P_{n2}^m(\mu)\, d\mu = \begin{cases} 1 \text{ for } n_1 = n_2 \\ 0 \text{ for } n_1 \neq n_2 \end{cases} \quad (6)$$

$$\frac{1}{2\pi} \int_0^{2\pi} \int_{-1}^{1} Y_{n1}^{m1}(\mu, \lambda) \cdot Y_{n2}^{*m2}(\mu, \lambda)\, d\mu\, d\lambda$$

$$= \begin{cases} 1 \text{ for } (m_1, n_1) = (m_2, n_2) \\ 0 \text{ for } (m_1, n_1) \neq (m_2, n_2) \end{cases} \quad (7)$$

These orthogonality conditions do not necessarily hold good for a hemispheric domain. It can however be shown that members of a set of associated Legendre functions having either odd or even number of zeros are orthogonal to each other over the hemisphere. Thus for a hemisphere we get a more specialised orthogonality condition

$$\int_{-1}^{1} P_{n1}^m(\mu) \cdot P_{n2}^m(\mu)\, d\mu = \begin{cases} 1 \text{ for } n_1 = n_2 \\ 0 \text{ for } n_1 \neq n_2 \end{cases} \quad (8)$$

where n_1-m and n_2-m are either both even or odd. $P_n^m(\mu)$'s in (8) are $\sqrt{2}$ times their corresponding values in (6). A similar modification applies to the orthogonality condition (7) for spherical harmonics over a hemisphere.

Using these orthogonality conditions, a given scalar field over the hemisphere may be analysed in terms of spherical harmonic components which are either symmetric or antisymmetric with respect to equator. Which of these two types of analyses should be applied to a given field is, however, to be dictated by the physical considerations.

The actual procedure for analysis has two stages :

(*i*) Fourier analysis of data along latitude circles upto desired order m.

(*ii*) Analysis of Fourier amplitudes in terms of desired number of associated Legendre function of first kind.

If $a_m(\theta)$ and $b_m(\theta)$ are the amplitudes of cosine and sine waves of order m along latitude θ, then utilising orthogonality condition (8), the real amplitudes of spherical harmonics of order m and degree n are given by :

$$a_n^m = \int_0^1 a_m(\theta)\, P_n^m(\mu)\, d\mu$$

$$b_n^m = \int_0^1 b_m(\theta)\, P_n^m(\mu)\, d\mu \quad (9)$$

Like Fourier components the complex and real amplitudes of spherical harmonics are related as

$$A_n^m = \frac{a_n^m - i\, b_n^m}{2} \quad \text{for } m \neq 0$$

$$A_n^0 = a_n^0 - i\, b_n^0 \quad \text{for } m = 0 \quad (10)$$

For the analysis under stage (*ii*) above by use of orthogonality condition, it is necessary to have values of Fourier amplitudes at different latitudes extending from equator to the north pole. The geopotential data analysed were picked up at 5° latitude-longitude intervals from 10° to 80 °N. The mean heights at equator and pole as well as at 5°N and 85°N were also estimated from the charts iteself. The Fourier amplitudes of different wave components were assumed to be zeros at equator and pole and those at 5°N and 85 °N as half of the amplitudes at 10 °N and 80°N, respectively. It was also assumed that the zonal component of wind is symmetric with respect to equator and consistent with this assumption the geopotential field was analysed in terms of a parallelogrammic truncated series of 112 symmetric spherical harmonics with $m \leqslant 15$ and $n-m$ having values 0, 2, 4....., 12. Such a constraint is necessary in the absence of data from the other hemisphere.

Numerical quadrature based on Simpson's rule was used for evaluating integrals on the right hand side of (9).

The values of associated Legendre function needed for the analysis were calculated for 0° to 90° N at 5° latitude intervals using the following recurrence formulae :

$$P_m^m = \left(1 + \frac{1}{2m}\right)^{1/2} \sqrt{1-\mu^2}\; P_{m-1}^{m-1}$$

$$P_n^m = \left(\frac{4n^2-1}{n^2-m^2}\right)^{1/2} \mu P_{n-1}^m - \left[\frac{(2n+1)(n-m-1)(n+m-1)}{(2n-2)(n^2-m^2)}\right]^{1/2} P_{n-2}^m \quad (11)$$

with starting value :

$$P_0^0 = \frac{1}{\sqrt{2}}$$

The progress of computations for generation of P_n^m's is schematically shown in Fig. 1. For a particular value of θ, starting with $P_0^0 = 1/\sqrt{2}$ the value of P_m^m for any m can be calculated from first formula with computations proceeding along diagonal line OA. Remembering that $P_n^m = 0$ for $n < m$, the second formula is used thereafter to compute P_n^m's having fixed value of m and successively increasing value of n. The computations for this purpose proceed along line parallel to n-axis. The progress of computations for function P_n^8 for n varying from 8 to 20 is shown in the figure by arrows.

As a check, the values of P_n^m's calculated above were compared with those given by Belousov (1962) and were found to agree with them. Before further use, these functions were multiplied by $\sqrt{2}$ to make them orthonormal over hemispheric domain.

3. Spectral form of linear balance equation

Linear balance equation

$$\nabla \cdot (f \nabla \Psi) = \nabla^2 \phi \quad (12)$$

can be used to obtain Ψ field from a given ϕ field.

An examination of expressions on the both sides of (12) shows that if ϕ is represented in terms of spherical harmonics symmetric with respect to equator, Ψ should be expanded in terms of spherical harmonic functions antisymmetric with respect to equator.

Thus ϕ and Ψ fields may be written as

$$\phi = \sum_{m=-M}^{M} \sum_{n=|m|,2}^{|m|+\mathbf{J}_2} \phi_n^m Y_n^m$$

$$\Psi = \sum_{m=-M}^{M} \sum_{n=|m|+1,2}^{|m|+\mathbf{J}_1} \Psi_n^m Y_n^m \quad (13)$$

where $\mathbf{J}_2$ is an even integer and $\mathbf{J}_1$, an odd and the summation over index n is at the interval of 2.

Substituting (13) in (12) and integrating both sides of the resulting equation over a hemispherical domain, we get the spectral form of linear balance equation as (for details see Appendix).

$$(n-1)(n+1)\beta_n^m \Psi_{n-1}^m + n(n+2)\alpha_n^m \Psi_{n+1}^m = \frac{n(n+1)}{2\Omega} \phi_n^m \quad (14)$$

where $\alpha_n^m = \left[\frac{(n+m+1)(n-m+1)}{(2n+1)(2n+3)}\right]^{1/2}$

$$\beta_n^m = \left[\frac{(n+m)(n-m)}{(2n-1)(2n+1)}\right]^{1/2}$$

and Ψ_n^m and Φ_n^m are the amplitudes of stream function and geopotential fields respectively. We adopt the truncation configuration of stream function as

$$0 \leqslant |m| \leqslant M = 15$$

$$n - |m| = 1, 3, 5, \ldots, \mathbf{J}_1 = 13$$

and of geopotential as

$$0 \leqslant |m| \leqslant M = 15$$

$$n - |m| = 0, 2, 4, \ldots, \mathbf{J}_2 = 12$$

Relation (14) consists of a set of linear algebric equations with number of dependent variables one more than the number of equations. However, a β_m^m as well as Ψ_{m-1}^m are equal to zero, (14) reduces to the following closed set of 7 algebric equations for each m, as shown in Eq. (15).

Starting with the first equation, the above system of equations can be solved easily to give stream function spectrum from the geopotential spectrum. However for $m=0$, both sides of the first of these equations vanish identically resulting in a singular solution for Ψ_1° and the system cannot be solved. This difficulty can be overcome in two possible ways :

(*i*) The first equation giving the singular solution may be excluded and instead one more equation of a higher degree added at the end of above system of equations. This requires the truncation of zonal harmonic spectrum of geopotential at Φ_{14}° instead of at Φ_{12}°. Assuming $\Phi_{15}^\circ = 0$ as the upper spectral boundary condition, we now get a closed system of equations which can be solved easily by building a solution from the lower to higher degree harmonics. By this procedure, however, the initial spectral boundary error magnifies taking alternatively

$$
\begin{vmatrix}
\tilde{\alpha}^m_m & 0 & 0 & 0 & 0 & 0 & 0 \\
\tilde{\beta}^m_{m+2} & \tilde{\alpha}^m_{m+2} & 0 & 0 & 0 & 0 & 0 \\
0 & \tilde{\beta}^m_{m+4} & \tilde{\alpha}^m_{m+4} & 0 & 0 & 0 & 0 \\
0 & 0 & \tilde{\beta}^m_{m+6} & \tilde{\alpha}^m_{m+6} & 0 & 0 & 0 \\
0 & 0 & 0 & \tilde{\beta}^m_{m+8} & \tilde{\alpha}^m_{m+8} & 0 & 0 \\
0 & 0 & 0 & 0 & \tilde{\beta}^m_{m+10} & \tilde{\alpha}^m_{m+10} & 0 \\
0 & 0 & 0 & 0 & 0 & \tilde{\beta}^m_{m+12} & \tilde{\alpha}^m_{m+12}
\end{vmatrix}
\begin{vmatrix} \Psi^m_{m+1} \\ \Psi^m_{m+3} \\ \Psi^m_{m+5} \\ \Psi^m_{m+7} \\ \Psi^m_{m+9} \\ \Psi^m_{m+11} \\ \Psi^m_{m+13} \end{vmatrix}
=
\begin{vmatrix} \tilde{\phi}^m_m \\ \tilde{\phi}^m_{m+2} \\ \tilde{\phi}^m_{m+4} \\ \tilde{\phi}^m_{m+6} \\ \tilde{\phi}^m_{m+8} \\ \tilde{\phi}^m_{m+10} \\ \tilde{\phi}^m_{m+12} \end{vmatrix} \qquad (15)
$$

where $\tilde{\alpha}^m_n = n(n+2)\ \alpha^m_n$

$$\tilde{\beta}^m_n = (n-1)(n+1)\,\beta^m_n$$

$$\tilde{\phi}^m_n = \frac{n(n+1)}{2\Omega}\ \phi^m_n$$

positive and negative signs as it propagates from the lower to higher harmonics (Merilees 1966).

(*ii*) The value of Ψ_1° may be obtained on the basis of some physical considerations. Using this as the lower spectral boundary condition and after dropping the first equation, the system (15) can be solved easily.

Ψ_1° and mean relative momentum M can be shown to be related as

$$\Psi^0_1 = -\frac{\sqrt{3}}{2}\,\overline{M} \qquad (16)$$

(*See* Appendix)

The mean relative momentum can be obtained from mean geostrophic wind calculated at different latitudes and thus Ψ_1° may be evaluated. Eliasen and Machenhauer (1965) used this procedure to circumvent the problem of singular solution. In this case, unlike procedure (*i*), any error in the initial estimate of Ψ_1° dampens taking alternating signs as the solution proceeds from the lower to the higher degree harmonics (Fig. 2). As may be seen the error in Ψ_1° reduces to about one-fourth in Ψ_5° and to as low as to one-tenth in Ψ_{13}°. Thus the second procedure is relatively superior to the first one and is adopted for spectral solution of balance equation. A comparison between the zonal mean geostrophic wind and zonal mean wind calculated at different latitudes from the stream function spectrum thus calculated is given in Table 1. The zonal mean wind obtained from stream function spectrum is found to be in agreement with zonal mean geostrophic wind to a high degree of accuracy over all the latitudes. The zonal wind based on stream function calculated by procedure (*i*) has been found to be in poor agreement with the zonal mean geostrophic wind at the higher and the lower latitudes (Merilees 1966).

4 An example of effectiveness of spherical harmonics in representing geopotential and stream function fields

To illustrate the efficiency of surface spherical harmonics in representing the hemispheric geopotential and stream function fields we consider

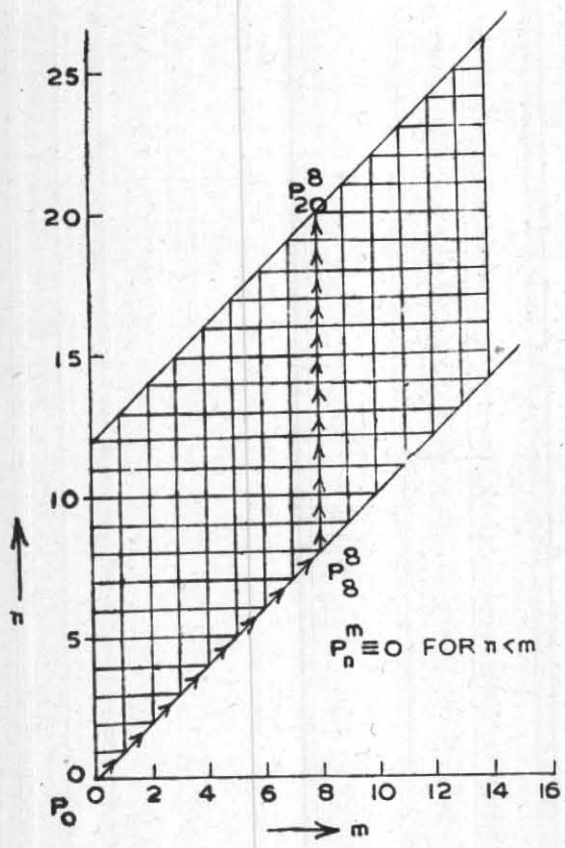

Fig. 1. Scheme for generation of associated Legendre functions

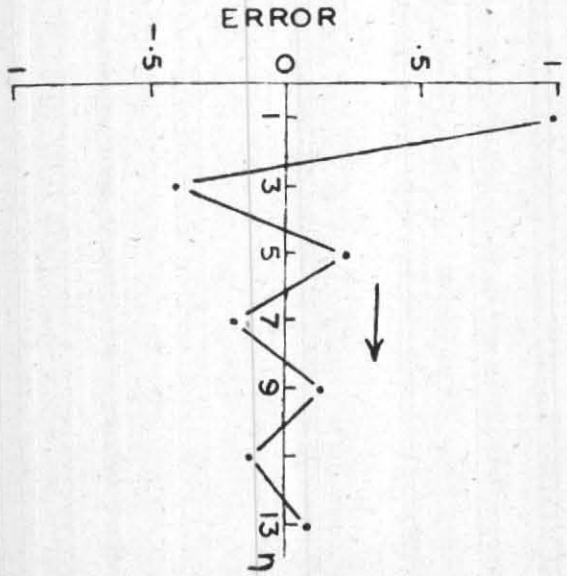

Fig. 2. Propagation of spectral boundary error

the 500 mb flow patterns of 1 January 1969. Fig. 3 shows the actual geopotential field while Fig. 4 has been arrived at by recombining 112 spherical harmonic components into which the actual geopotential field was analysed. Fig. 5 is based on combination of different components of stream function spectrum corresponding to geopotential spectrum representing Fig. 4.

The circulation patterns (Fig. 3) are the typical ones for the mid-troposphere during winter season. A well marked low pressure area lies over Central Asia extending east-west through China and neighbourhood with two centres — one near 80°E/50°N and the other north of the Sea of Japan near 135° E/45°N. A low pressure area to the north of Alaska is the centre of Polar cap low. A well marked trough runs from Alaska to North Pacific Ocean upto about 165°E/30°N. Another shallow centre of polar-cap low lies over Greenland with two well

TABLE 1

Comparison between 500 mb mean zonal geostrophic wind and mean zonal wind calculated from stream function spectra

Lat. (°N)	July 1968 $\bar{U}_g$	July 1968 $\bar{U}_\psi$	January 1969 $\bar{U}_g$	January 1969 $\bar{U}_\psi$
0	—0·4	0·0	0·6	1·3
5	—1·4	—1·2	1·7	2·2
10	—4·4	—3·7	5·6	4·8
15	—5·3	—5·4	8·9	8·6
20	—4·1	—4·5	13·0	12·9
25	—0·5	—0·8	17·0	16·8
30	4·1	4·1	19·8	19·6
35	8·2	8·2	20·2	20·2
40	10·3	10·2	18·3	18·5
45	10·3	10·2	14·6	14·8
50	8·8	8·8	10·2	10·3
55	6·8	7·0	6·4	6·4
60	5·1	5·1	3·8	3·8
65	3·7	3·6	2·3	2·4
70	2·5	2·4	1·6	1·7
75	1·6	1·6	1·3	1·3
80	0·7	0·9	0·9	0·8
85	0·4	0·5	0·5	0·4

$\bar{U}_g$ mean zonal geostrophic wind

$\bar{U}_\psi$ mean zonal ψ wind with boundary condition

$\psi_1^\circ = -(\sqrt{3}/2)\bar{M}$ unit : m sec^{-1}

marked troughs—one over North Atlantic Ocean along about 50°W and the other over West Europe. A well marked low pressure area over East Canada has a trough running upto Gulf of Maxico. Well marked ridges lie between East-Central Asia and Alaska low pressure systems as well as between the ow pressure area over West-Central Asia and the trough over West Europe. An extensive high pressure area centred near 20°W/50°N lies over

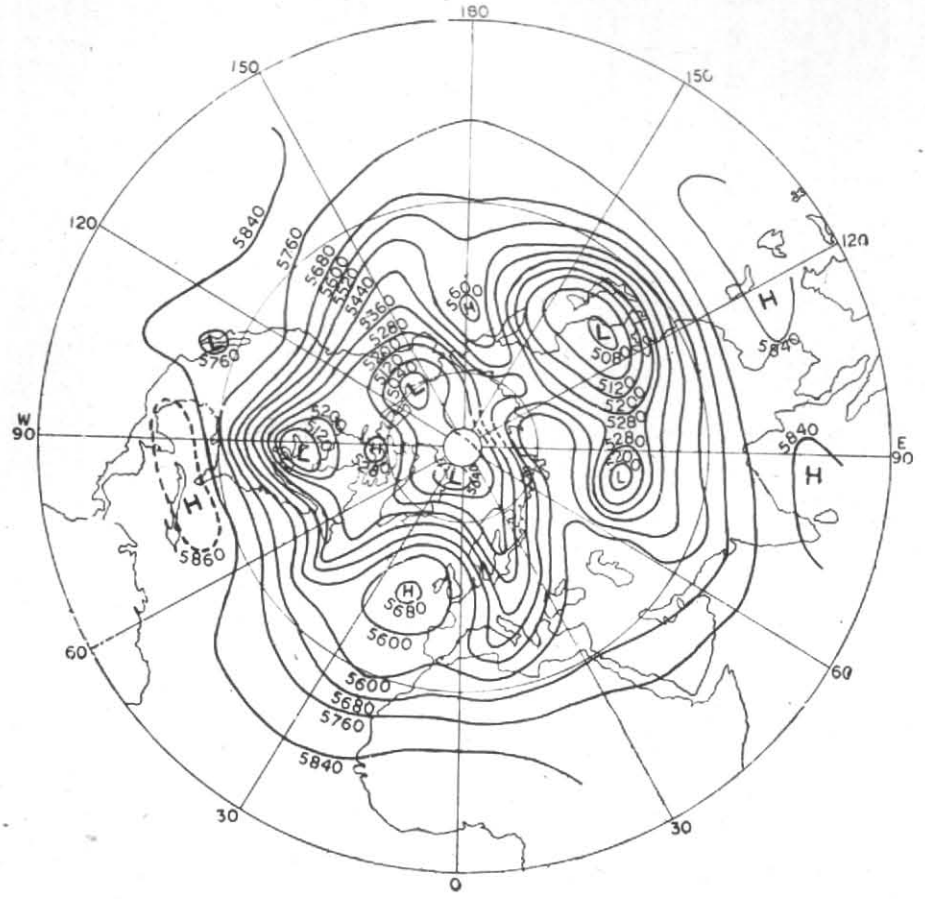

Fig 3 500 mb geopotential filed of January 1969

TABLE 2

Percentage of total variance explained by different spherical harmonics in representation of 500 mb chart of 1 January 1969

m	$n-m$							
	0	2	4	6	8	10	12	Total
0	—	75·76	0·95	0·17	1·70	0·01	0·08	78·67
1	1·14	0·87	3·63	1·11	0·03	0·02	0·06	6·86
2	0·23	1·51	0·53	2·06	0·88	0·03	0·02	5·26
3	0·04	1·06	0·72	0·03	0·11	0·01	0·01	1·98
4	0·00	0·18	0·69	0·27	0·28	0·12	0·01	1·55
5	0·06	0·43	0·52	0·37	0·06	0·03	0·01	1·48
6	0·07	0·69	0·62	0·16	0·03	0·00	0·01	1·58
7	0·00	0·12	0·23	0·06	0·01	0·01	0·00	0·43
8	0·01	0·01	0·03	0·01	0·05	0·04	0·00	0·15
9	0·00	0·00	0·09	0·08	0·01	0·00	0·00	0·18
10-15	0·00	0·03	0·09	0·07	0·02	0·01	0·00	0·22
Total	1·55	80·66	8·10	4·39	3·18	0·28	0·20	98·36

NOTE—0·00 means less than 0·005

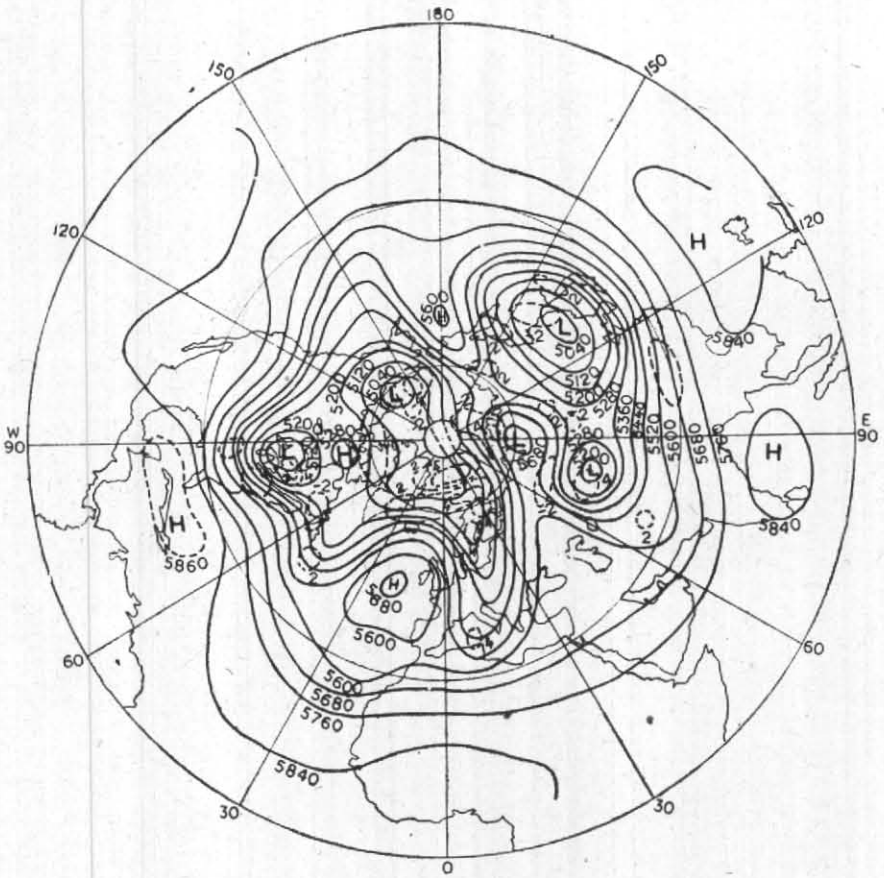

Fig. 4. 500 mb geopotential field constructed from spherical harmonic components of 1 January 1969
Contour heights in metres, difference between actual and fitted contours heights in tens of metres.

North Atlantic Ocean and is flanked by troughs to its east and west. Among the low latitude systems a well marked trough lies to the west of Maxico. A shallow trough lies to the west of Africa. Another shallow trough extending from the north lies over Arabian Sea. Sub-tropical high has its axis running between 10°N and 15°N over Asia and between 20°N and 25°N over western half of north Atlantic Ocean. Centres of high pressure cells lie over Bay of Bengal, Phillipine Sea and North-West Atlantic Ocean.

An examination of Fig. 4 shows that the above systems have been brought out very well by spherical harmonics representation. The areas having differences between fitted and the actual geopotential values of 20 gpm or more are also marked in this figure. We see that the differences of this order appear generally near well marked centres of high and low pressure systems and troughs and ridges. The higher differences are mostly to the north of 70°N. The fitted values are generally slightly higher near low pressure areas and slightly lower near high pressure areas thus smoothening out the actual patterns to some extent. The contribution of each harmonic in representing this geopotential field can be seen from Table 2 which shows the percentage variance explained by different harmonics. All the components together explain more than 98 per cent of the total variance out of which 78·7 per cent is explained by 6 zonal harmonics alone.

From Fig. 5, we may see that the stream function patterns are very similar to the geopotential patterns of Fig. 4. The centres of lows and highs and positions of troughs and ridges of geopotential field have been brought out very well. Somewhat weak gradients in the isolines of stream function in comparison to contour height gradients of Fig. 4 are due to the fact that the interval of 1×10^6 m^2 sec^{-1} between stream function isolines in this figure corresponds approximately to 90 gpm whereas analysis in Fig. 3 and Fig. 4 is at a closer interval of 80 gpm.

5. Conclusions

Besides the physical and computational formulations of the model atmosphere, the initial

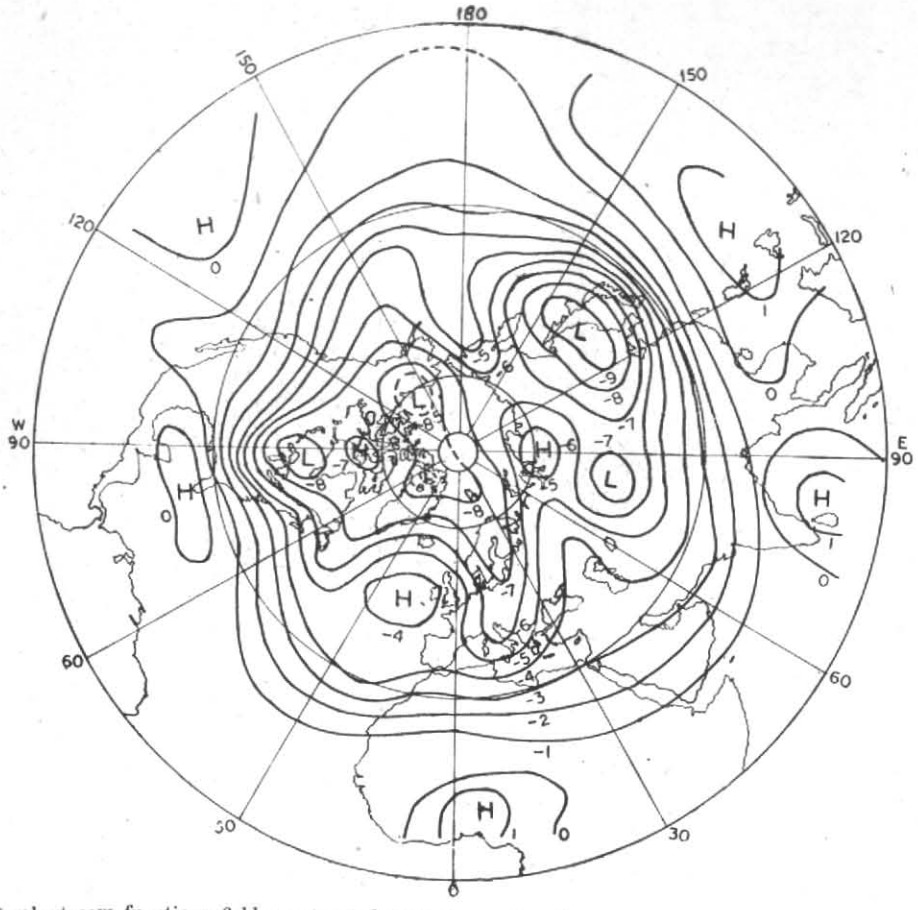

Fig. 5. 500 mb stream functions field constructed from stream function spectral components of 1 January 1969

input plays an important role in the quality of final results of diagnostic or prognostic atmospheric models. Equispaced grid point data based on objective or subjective analysis forms an accepted way of providing input for these numerical models. In the case of spectral models, the initial input is required to be in the form of amplitudes of different meteorological fields. One of the common input in these models is the geopotential height or the stream function derived from it. The purpose of present study was to demonstrate the method for transforming these fields from space domain into spectral domain. A comparison between the actual geopotential fields and that based on spectral representation has shown that the large scale hemispheric flow patterns can be represented to a high degree of accuracy in terms of a relatively limited number of harmonic components. The stream function spectrum derived from the spectral solution of linear balance equation also gives a proper representation of the actual flow patterns. The centres of synoptic systems are well brought out in the geopotential as well as in the stream function field based on spectral representation. The spectral representation, however, smoothens the small and intense systems to some extent. As in the case of extended area (hemisphere) models the interest lies more in the large scale systems, such smoothening of input is more often desirable than not. Thus the above scheme can be used effectively to provide a sitable input for a spectral model. The work on such model is already in progress.

Acknowledgement

The author is thankful to the Director General of Observatories, New Delhi for providing facilities for this work. The encouragement received during the course of study from Dr. K.R. Saha, Director, Indian Institute of Tropical Meteorology, Poona, Dr. P.K. Das, Deputy Director General of Observatories, New Delhi and Dr. P. S. Pant, Director, N.H.A.C., New Delhi is gratefully, acknowledged.

REFERENCES

Belousov, S. L.	1962	*Tables of normalised associated Legeedre Polynomials* (translated from the Russian). Pergamon Press, 379 pp.
Bourke, W.	1972	*Mon. Weath. Rev.*, **99**, pp. 683-689.
Eliasen, E. and Machenhauer, B.	1965	*Tellus*, **17**, pp. 220-238.
Eliasen, E., Machenhaur, B. and Rasmussen, E	1970	On a numerical method for integration of the hydrodynamical equations with spectral representation of horizontal fields. Inst. Theoretical Met. Univ. Copenhgen, Rep. No. 2, p 35
Kurbatkin, G. P.	1972	*Telus*, **24**, pp. 499-513.
Lorenz, E. N.	1963	*J. Atmos. Sci.*, **20**, pp. 448-464.
Merilees, P.	1966	Harmonic representation applied to large scale atmospheric waves. McGill Univ. Sci. Rep. No. 3, 174. pp.
Orszag, S. A.	1970	*J. Atmos. Sci.* **27**, pp. 890-895.
Robert, A. J.	1966	*J. Met. Soc. Japan*, Ser. 2, 44, pp. 237-245.
Saltzman, B. and Fleisher, A.	1960	*Tellus*, **12**, pp. 374-377.
Wiin-Nielsen, A.	1964	Some new observational studies of energy and energy transformation in the atmosphere *WMO Tech. Note* No. 66, pp. 177-202.
	1967	*Tellus*, **19**, pp. 540-559.
W.M.O., Geneva.	1974	Hemispheric 4-level spectral model. Modelling for the first GARP Global Experiment, GARP publ. No. 14, pp 218-225.

APPENDIX

1. Derivation of spectral form of linear balance equation

We write linear balance equation (12) as

$$f \nabla^2 \Psi + \nabla f \cdot \nabla \Psi = \nabla^2 \phi \tag{A.1}$$

We shall make use of recurrence formulae

$$\sin\theta P_n^m = a_n^m \; P_{n+1}^m + \beta_n^m \; P_{n-1}^m \tag{A.2}$$

$$\text{and } \cos\theta \frac{d P_n^m}{d\theta} = -n a_n^m \; P_{n+1}^m + (n+1) \; \beta_n^m \; P_{n-1}^m \tag{A.3}$$

$$\text{where } a_n^m = \left[\frac{(n+m+1)(n-m+1)}{(2n+1)(2n+3)}\right]^{1/2}$$

$$\beta_n^m = \left[\frac{(n+m)(n-m)}{(2n-1)(2n+1)}\right]^{1/2}$$

$$\text{and } \beta_n^m = a_{n-1}^m$$

for transforming (A·1) into its spectral form.

On substituting spectral expression for Ψ and ϕ in different terms of (A·1) we get

$$f \nabla^2 \Psi = -\frac{2\Omega}{a^2} \sin\theta \sum_{m=-M}^{M} \sum_{n=|m|+1,2}^{|m|+J_1} n(n+1) \; \Psi_n^m \; Y_n^m$$

$$= -\frac{2\Omega}{a^2} \sum_{m=-M}^{M} \sum_{n=|m|,2}^{|m|+J_2} n(n+1) \; \Psi_n^m \left(a_n^m \; Y_{n+1}^m + \beta_n^m \; Y_{n-1}^m \right)$$

[using (A.2)]

$$= -\frac{2\Omega}{a^2} \sum_{m=-M}^{M} \sum_{n=|m|,2}^{|m|+J_2} \left[(n+1)(n+2) a_n^m \; \Psi_{n+1}^m + n(n-1) \beta_n^m \; \Psi_{n-1}^m \right] Y_n^m \tag{A.4}$$

$$\nabla f \,.\, \nabla \Psi = \frac{2\,\Omega \cos\theta}{a^2} \sum_{m=-M}^{M} \sum_{n=|m|+1,\,2}^{|m|+J_1} \Psi_n^m \frac{d\,Y_n^m}{d\,\theta}$$

$$= \frac{2\,\Omega}{a^2} \sum_{m=-M}^{M} \sum_{n=|m|,\,2}^{|m|+J_1} \Psi_n^m \left(-n\,a_n^m\,Y_{n+1}^m + (n+1)\,\beta_n^m\,Y_{n-1}^m \right)$$

[using (A.3)

$$= \frac{2\,\Omega}{a^2} \sum_{m=-M}^{M} \sum_{n=|m|,\,2}^{|M|+J_2} \left[(n+2)\,a_n^m\,\Psi_{n+1}^m - (n-1)\,\beta_n^m\,\Psi_{n-1}^m \right] Y_n^m \tag{A.5}$$

$$\nabla^2 \phi = -\sum_{n=-M}^{M} \sum_{n=|m|,\,2}^{|m|+J_2} \frac{n\,(n+1)}{a^2}\,\phi_n^m\,Y_n^m \tag{A.6}$$

From (A·1) and (A·4) to (A·6) we get

$$2\,\Omega \sum_{m=-M}^{M} \sum_{n=|m|,\,2}^{|m|+J_2} \left[n\,(n+2)\,a_n^m\,\Psi_{n+1}^m + (n-1)\,(n+1)\,\beta_n^m\,\Psi_{n-1}^m \right] Y_n^m$$

$$= \sum_{m=-M}^{M} \sum_{n=|m|,\,2}^{|m|+J_2} n\,(n+1)\,\phi_n^m\,Y_n^m \tag{A.7}$$

Multiplying both sides of equation (A·7) by Y_n^{*m} and integrating over hemispherical domain we get the spectral form of linear balance equation as :

$$(n-1)\,(n+1)\,\beta_n^m\,\Psi_{n-1}^m + n\,(n+2)\,a_n^m\,\Psi_{n+1}^m = \frac{n\,(n+1)}{2\,\Omega}\,\phi_n^m \tag{A.8}$$

2. Relation between $\bar{M}$ and Ψ_1°

Mean relative angular momentum is given by

$$\bar{M} = \frac{1}{2\pi a^2} \int_0^{2\pi} \int_0^{\pi/2} (U\,a\cos\theta)\,a^2 \cos\theta\; d\theta \,.\, d\lambda \tag{A.9}$$

$$= \frac{1}{2\pi} \int_0^{2\pi} \int_0^{\pi/2} \left(-\frac{\partial \Psi}{\partial \theta} + \frac{\partial \chi}{\cos\theta\,\partial \lambda} \right) \cos^2\theta\, d\,\theta\, d\,\lambda$$

As the second term vanishes on integration along λ, we get in terms of spectral expansion of Ψ,

$$\overline{M} = \frac{1}{2\pi}\int_0^{2\pi}\int_0^{\pi/2} - \sum_{m=-M}^{M} \sum_{n=|m|+1,2}^{|m|+J_1} \Psi_n^m \left(\cos\theta \frac{dP_n^m}{d\theta} \right) \cos\theta\, e^{im\lambda}\, d\theta\, d\lambda$$

Clearly the above integral vanishes except for $m=0$, in which case it gives

$$\overline{M} = \int_0^{\pi/2} - \sum_{n=1,2}^{J_1} \Psi_1^0 \left(\cos\theta \frac{dP_n^o}{d\theta} \right) \cos\theta\, d\theta$$

$$= -\int_0^{\pi/2} \sum_{n=1,2}^{J_1} \Psi_1^0 \left(-n\alpha_n^o P_{n+1}^o + (n+1)\beta_n^o P_{n-1}^o \right) \cos\theta\, d\theta$$

[using (A.3)]

Due to orthogonality condition (8), the integral on the right hand side, except that involving P_0^0 vanish, so that

$$\overline{M} = -2\beta_2^0 \Psi_1^0 = -\frac{2}{(3)^{1/2}} \Psi_1^0$$

or $$\Psi_1^0 = -\frac{(3)^{1/2}}{2}\overline{M} \qquad \text{(A.10)}$$